MRS Communications (2013), *3*, 31–36
© Materials Research Society, 2013
doi:10.1557/mrc.2013.7

MRS Communications

Research Letters

Phonon drag effect in nanocomposite $FeSb_2$

Mani Pokharel, Huaizhou Zhao, Kevin Lukas, Zhifeng Ren, and **Cyril Opeil,** Department of Physics, Boston College, Chestnut Hill, Massachusetts 02467
Bogdan Mihaila, Los Alamos National Laboratory, Los Alamos, New Mexico 87545
Address all correspondence to Mani Pokharel at **pokharem@bc.edu**

(Received 15 November 2012; accepted 1 February 2013)

Abstract

We study the temperature dependence of thermoelectric transport properties of four $FeSb_2$ nanocomposite samples with different grain sizes. The comparison of the single crystals and nanocomposites of varying grain sizes indicates the presence of substantial phonon drag effects in this system contributing to a large Seebeck coefficient at low temperature. As the grain size decreases, the increased phonon scattering at the grain boundaries leads to a suppression of the phonon-drag effect, resulting in a much smaller peak value of the Seebeck coefficient in the nanostructured bulk materials. As a consequence, the ZT values are not improved significantly even though the thermal conductivity is drastically reduced.

Introduction

Owing to its unusual magnetic and electronic transport properties, the narrow-gap semiconductor $FeSb_2$ has been one of the extensively studied compounds in the past few decades.[1–4] The renewed interest in this compound came after Bentien et al.[5] reported a colossal value of the Seebeck coefficient of –45,000 μV/K with a record high value of the power factor (PF) of 2300 $\mu W/K^2/cm$ at around 10 K in single crystal samples, which may make this material a potential candidate for the Peltier cooling applications at very low temperature near 10 K. Despite the huge PF value, the dimensionless figure of merit (ZT) values for single crystal samples are limited by a very high thermal conductivity $\kappa \sim 500$ W/m/K at ~10 K. In our earlier work,[6] we were able to reduce the thermal conductivity by three orders of magnitude to 0.5 W/m/K in achieving a peak ZT value of ~0.013 at ~50 K in nanocomposite samples. However, the Seebeck coefficient in the nanocomposites is severely degraded at low temperatures when compared with that of the single crystal counterpart. For optimized samples with $\kappa = 0.40$ W/m/K and $\rho = 1.2 \times 10^{-4}$ Ω m at 50 K, a Seebeck coefficient of –970 μV/K is required to achieve a ZT value of 1. Unfortunately, the measured value of the Seebeck coefficient at 50 K was only –109 μV/K. Therefore, it is important to know the origin of the large Seebeck coefficient in this system to further improve ZT.

The classical theory of thermoelectricity is based on the assumption that the flow of charge carriers and phonons can be treated independently. Under this assumption, the Seebeck coefficient arises due solely to spontaneous electron diffusion. However, when the two flows are linked, the effect of electron–phonon scattering should be taken into account. Hence, in general, the Seebeck coefficient is given as the sum of two independent contributions[7]

$$S = S_d + S_p, \quad (1)$$

where S_d is the conventional electron-diffusion part and S_p is the phonon-drag contribution. The diffusion part is caused by the spatial variation of the electronic occupation in the presence of a thermal gradient, whereas the drag part arises due to the interaction between anisotropic lattice vibrations and mobile charge carriers. Herring[7] showed that the higher than expected value of thermopower in germanium[8] and other semiconductors could be explained assuming that the carriers are preferentially scattered by the phonons toward the cold end of the sample. The dragging of some of the charge carriers along the thermal gradient gives rise to an additional thermoelectric electromotive force (emf). Because the additional emf and the emf induced by diffusion have the same sign, the overall phonon-drag effect is to increase the Seebeck coefficient. Generally, this effect becomes stronger at lower temperatures where the phonon mean free path becomes longer.

The origin of the colossal Seebeck coefficient in $FeSb_2$ at low temperature is not completely understood yet. Several authors[5,9–12] suggested a strong electron–electron correlation as a possible cause. Other authors,[13,14] however, surmised that the origin of the colossal value of the Seebeck coefficient is not due to electron–electron correlations but due to the phonon drag effect. In this paper, we study the thermoelectric properties of $FeSb_2$ nanocomposites and present evidence of

https://doi.org/10.1557/mrc.2013.7 Published online by Cambridge University Press

a substantial phonon-drag contribution to the Seebeck coefficient in $FeSb_2$.

Experimental

Nanostructured $FeSb_2$ samples were synthesized by first forming an ingot through melting and solidification. The ingot was ball milled and hot pressed at different temperatures to obtain the nanocomposite samples with different grain sizes ranging from nanometers to micrometers. The labels given to the different samples and the corresponding processing parameters are shown in Table I. The Seebeck coefficient (S), electrical resistivity (ρ), thermal conductivity (κ), and Hall coefficient (R_H) were measured on a Physical Property Measurement System (PPMS) from Quantum Design Inc. (San Diego, CA). Sample preparation and measurements were performed in the manner described in Ref. 6.

Results and discussions

Figure 1 shows the temperature dependence of the Seebeck coefficient for our four nanocomposite samples. Sample S-600 was measured both in magnetic fields of 0 and 9 T. The Seebeck coefficients of all samples are significantly smaller than that of a single crystal at low temperature, whereas at high temperature the values are comparable. A room temperature value of $S \sim 26$ μV/K was observed for all our samples. This value is comparable to $S \sim 31$ μV/K reported for the single crystal.[15] A decrease in the Seebeck coefficient at low temperature in polycrystal,[11] thin films[16] and arsenic-substituted $FeSb_2$ single crystals[9] was reported earlier. As shown in the inset of Fig. 1, the peak value of the Seebeck coefficient (S_{max}) decreases with decreasing grain size. This is expected for the phonon-drag effect, because the non-electronic scattering (grain boundary scattering in the case of nanocomposites) reduces the phonon mean free path, which in turn decreases the phonon-drag contribution. A similar conclusion was drawn in Ref. 14. Yet another example of the reduction of phonon mean free path decreasing phonon drag contribution was shown by Weber et al.[17] It was demonstrated, using point contacts, that when the contact size becomes comparable to the mean free path of the relevant phonons, the phonon-drag part of the thermopower is suppressed by the boundary scattering. Here, we also note that the temperature profile of the Seebeck coefficient for the samples with larger grains follows the typical behavior of phonon-drag system as suggested by Blatt.[18]

Table 1. Assigned IDs, processing temperature, and average grain sizes estimated from the SEM images for the four nanocomposite $FeSb_2$ samples.

Sample code	Hot pressing temperature (°C)	Average grain size (nm)
S-300	300	30
S-400	400	100
S-500	500	350
S-600	600	20,000

The Seebeck peaks shift to the higher temperature when the grain size decreases (inset of Fig. 1). This type of size-dependent shift in the Seebeck peak is one of the characteristics of the phonon-drag-dominated systems, as pointed out previously.[8,19,20]

Usually, a small magnetothermopower is expected for the phonon-drag dominated system. For sample S-600 at 25 K, we observed a relative change in the Seebeck coefficient, $(S(9T) - S(0T))/S(0T) = 0.059$. This small value supports the non-electronic origin of the large Seebeck coefficient in this sample.

Figure 2 shows the temperature dependence of the thermal conductivity (κ) for the four samples. Calculations based on the Wiedemann–Franz law show that below 50 K, more than 97% of the total thermal conductivity comes from the lattice contribution. For large-grained samples, a temperature dependence of the form $\kappa \sim T^2$ is nearly obeyed at temperatures below 50 K. Weber et al.[21] reported a similar T^2 behavior in silicon below 20 K that they attribute to strong electron-phonon scattering. As the grain size decreases, we find a gradual deviation from the T^2 law. This can be understood as follows: for a large-grained sample, the number of available phonons interacting with the carriers is large which causes significant phonon-drag. As the grain size decreases the number of relevant phonons decreases and as a result the preferential scattering of electrons by phonons becomes weaker. Evidence for electron–phonon coupling in $FeSb_2$ single crystals was also reported by Perucchi et al.[22] who found a large change in phonon lifetimes using optical spectroscopy. Lazarevic et al.[23] later suggested that the electron–phonon coupling is temperature dependent below 40 K.

The inset of Fig. 2 shows the change in the Seebeck coefficient with thermal conductivity for 25 and 50 K. At 25 K, the Seebeck coefficient increases linearly with the thermal conductivity. The linear relationship is expected because in a phonon-drag dominated system S_p is expected to follow the same temperature dependence as the phonon heat capacity so that S_p and the lattice thermal conductivity (κ_l) are linearly related. This indicates that phonons play a significant role in determining the Seebeck coefficient values of our samples at around 25 K. At 50 K, however, the Seebeck coefficient decreases with increasing thermal conductivity without any obvious trend. This is an indication that the phonon-mean free path decreases and the phonon-drag effect becomes weak at higher temperature.

Significant phonon drag effects are expected to occur when the dominant phonons acquire sufficient momentum to scatter carriers across the Fermi surface.[24] In a rough approximation, $T_{max} \approx \frac{1}{10}\theta_D$, where T_{max} is the temperature at which the phonon drag peak occurs and θ_D is the Debye temperature. For rutile TiO_2,[25] θ_D is 450–780 K and the Seebeck peak occurs at 10–30 K. For bismuth,[20] another well-known

https://doi.org/10.1557/mrc.2013.7 Published online by Cambridge University Press

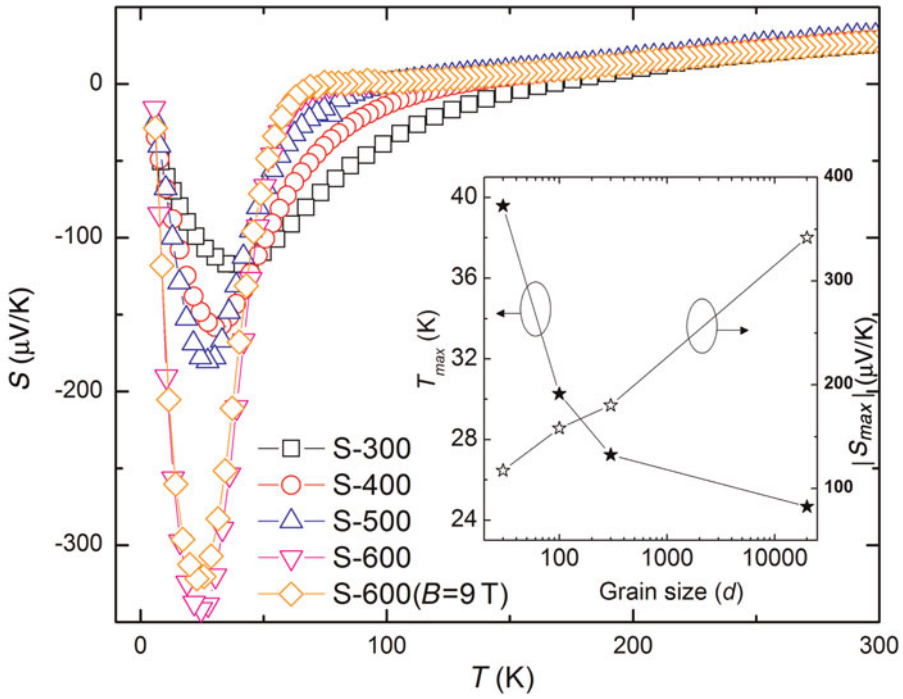


Figure 1. Temperature dependence of the Seebeck coefficient for the four samples. Sample S-600 was measured both at 0 and 9 T magnetic fields. Inset: The grain size dependence of the peak value (S_{max}) and the peak position (T_{max}) of the Seebeck coefficient.

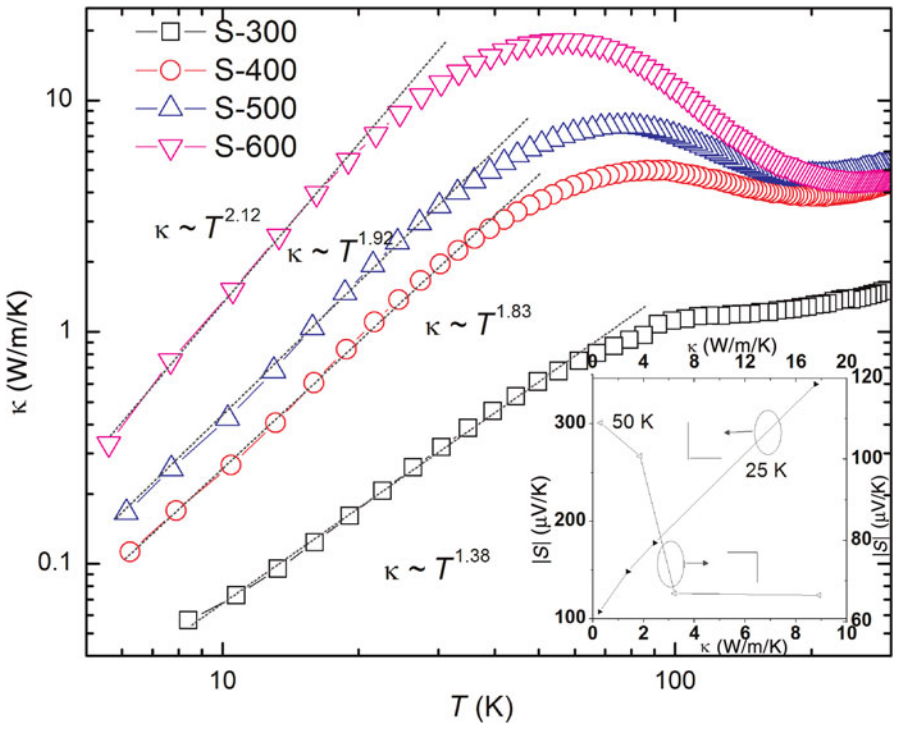


Figure 2. Temperature dependence of the thermal conductivity for the four samples. Fitting to the power law was done for all the samples below 50 K. Inset: Seebeck coefficient as a function of thermal conductivity at 25 and 50 K.

https://doi.org/10.1557/mrc.2013.7 Published online by Cambridge University Press

phonon drag system, θ_D is 119 K, whereas the Seebeck peak occurs at 2–3 K. For the $FeSb_2$ polycrystal, $\theta_D \approx 330 - 350$K was reported in Ref. 11 and 256 K in Ref. 26. The Seebeck peak in single crystal occurs at around 10 K. For our sample S-600, the peak occurs at 25 K. Hence, comparing with the other phonon drag systems, the scaling between T_{max} and θ_D in $FeSb_2$ is consistent with the phonon-drag picture.

Following Herring,[7] the electron-diffusion part of the Seebeck coefficient, in μV/K, for a semiconductor is given by

$$S_d = \mp 86.2\left[\ln\frac{4.7\times10^{15}}{n} + \frac{3}{2}\ln\frac{m^*}{m} + \frac{|\Delta E|}{kT} + \frac{3}{2}\ln T\right], \quad (2)$$

where n is the charge carrier density expressed in cm^{-3}, m and m^* are the bare and effective masses of the electron, respectively, and ΔE is the average energy of the transported electrons relative to the band edge. In Eq. (2), the upper and lower signs are for n-type and p-type materials, respectively.

For the case of lattice scattering by long wavelength phonons, $|\Delta E|/kT$ can be approximated by[7]

$$\left|\frac{\Delta E}{kT}\right| = \frac{5}{2} + r, \quad (3)$$

where the scattering parameter r is taken to be $-1/2$. S_d was calculated taking $m^* = m$ and using the charge carrier density (n) calculated from the Hall-coefficient measurements. The diffusion part was then subtracted from the total measured Seebeck coefficient to obtain the drag contribution shown in Fig. 3. For S-600 at 25 K, we find the diffusion value, $S_d = -110$ μV/K. Using Eq. (1), S_p was calculated to be -238 μV/K. However, for S-300 the calculated diffusion contribution turned out to be slightly larger than the measured values. Hence, no significant phonon drag contribution is expected for this sample. This is understandable, because the phonon mean free path for sample S-300 is drastically reduced so that the dominant phonons do not carry sufficient momentum to scatter carriers. Moreover, the phonon drag is expected to weaken with increasing carrier concentration and, in fact, it has been proposed that a saturation effect occurs at high concentration level. The overestimation of the diffusion part of the Seebeck coefficient in S-300 is probably due, in part, to the approximations made in the above calculations.

The phonon-drag thermopower for semiconductors, in the first-order approximation, can be written as[7]

$$S_p = \frac{\beta v_s \lambda_p n e}{\sigma T}, \quad (4)$$

where v_s is the velocity of sound, λ_p the mean free path of the interacting phonons, n the charge carrier density, σ the electrical conductivity, T is the absolute temperature, and β is the dimensionless parameter with its value ranging from 0 to 1 depending upon the strength of the interaction. Equation (4) can be used to find approximate values of the mean free path of t phonons interacting with the electrons. The mean free path of an average phonon can also be estimated from the lattice thermal conductivity based on kinetic theory[27]

$$K_l = \frac{1}{3} c_V \tilde{\lambda}_P v_S, \quad (5)$$

where K_l is the lattice thermal conductivity and c_V the phonon contribution to the total specific heat capacity. The lattice contribution of the total thermal conductivity was calculated assuming $\kappa_{total} = \kappa_l + \kappa_e$ and $\kappa_e = L\sigma T$, where κ_e is the electronic contribution to the total thermal conductivity. The Lorenz number in the free electron model, $L = 2.45\times10^{-8}$ $W/K^2/\Omega$ was used, c_V was calculated using $C_P - \gamma T = \beta T^3$ with $\gamma = 3.98\times10^{-3}/JK^2/mol$, as reported in Ref. 11, and the C_P values were obtained from the same reference. Figure 4 shows the temperature dependence of the two length scales for samples S-600. It turns out that with $\upsilon_s = 3116$ m/s and $\beta = 0.5$, the two length scales, which come from two independent calculations, are of the same order of magnitude and more importantly they behave roughly the same way as a function of temperature. This suggests that similar wavelength phonons are playing a role in both the thermal conductivity and the phonon-drag effect. A similar analysis was performed in Ref. 28 to describe the unusually large Seebeck coefficient in rutile TiO_2 at low temperature.

According to Keyes et al.[29] the value of the figure of merit (Z_p) that can be reached using phonon drag is rather low. Based on their argument, Goldsmid[30] shows that Z_pT is less than ¼ for a bulk thermoelectric material. Ivanov et al.[31] reported recently a similar conclusion for low-dimensional structures. These conclusions are consistent with our earlier work[6] where, despite the dramatic reduction in the thermal

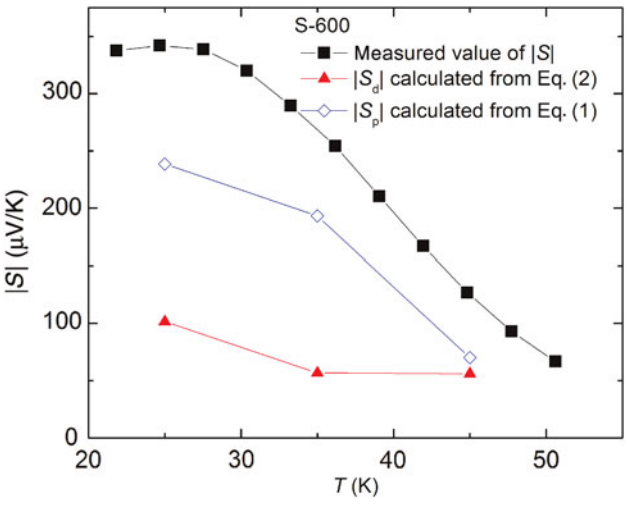


Figure 3. Temperature dependence of the calculated value of diffusion and drag part for the sample S-600 based on Eqs. (1) and (2). The carrier concentration obtained from the Hall coefficient data was used in the calculation. The measured total Seebeck coefficient is also plotted for comparison.

https://doi.org/10.1557/mrc.2013.7 Published online by Cambridge University Press

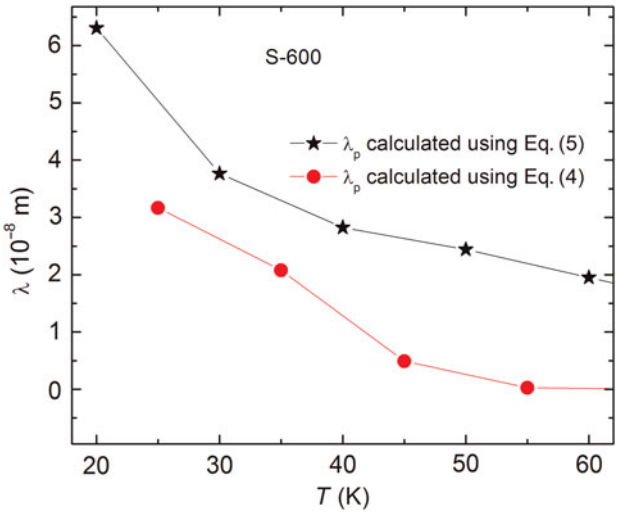


Figure 4. Temperature dependence of the phonon mean free paths calculated from two independent calculations using Eqs. (4) and (5).

conductivity by three orders of magnitude, *ZT* values were not improved significantly Fig. 3(d) in Ref. [6].

Finally, our nanocomposite data and analysis of phonon drag do not support other mechanisms that might explain the large Seebeck effects reported by Bentien et al.[5] Although one cannot preclude the presence of electron–electron correlation effects, their role in this phenomenon may be a minor one. The recent analysis of electron correlations using a hybrid functional approach of Becke[32] and Hegin's *GW* functional approach[33] by Tomczak et al.[14] suggest that the high thermopower in $FeSb_2$ should not be understood in the context of local correlations, but rather by utilizing vertex corrections to the transport coefficients. Such vertex corrections describe the phonon-drag effect. The phonon-drag effects in $FeSb_2$ are similar to those described in p-type Ge by Geballe and Hull.[8] In a similar vein the study of magnetoresistance and Hall effect by Takahashi et al.[13] concludes that the large Seebeck coefficient in $FeSb_2$ is unlikely to originate from electron–electron correlations because they have an insignificant effect on the Seebeck coefficient in the low-temperature insulating regime. Our data on $FeSb_2$ nanocomposite supports their conjecture that the phonon-drag effect plays an essential role in enhancing the Seebeck coefficient in the low-temperature regime, as shown in other semiconductor materials e.g., InSb[34] and weakly P doped Si.[21]

Conclusions

To summarize, in this paper we analyzed qualitatively and quantitatively several indicators of the presence of substantial electron–phonon interaction in $FeSb_2$ at low temperature. Our analysis indicates that a significant phonon-drag effect must take place in coarse-grained samples at low temperature. As the grain size decreases, the phonon drag effect becomes weaker, causing a much smaller peak value of the Seebeck coefficient in fine-grained samples. Based on these results we conclude that the phonon drag plays a significant role in the colossal value of the Seebeck coefficient in $FeSb_2$ single crystals. Therefore, the ZT values of $FeSb_2$ nanocomposite cannot be improved significantly even though the thermal conductivity can be drastically reduced.

Acknowledgments

The authors would like to thank J. Heremans, K. Kempa, and R. Farrell, S.J. for helpful discussions and comments on the manuscript. C.O. acknowledges financial support from the Trustees of Boston College. We gratefully acknowledge funding for this work by the Department of Defense, United States Air Force Office of Scientific Research, Multi-University Research Initiative (MURI) Program under Contract No. FA9550-10-1-0533.

References

1. H. Holseth and A. Kjekshus: Compounds with marcasite type of structure IV. The crystal structure of $FeSb_2$. *Acta Chem. Scand.* **23**, 3043 (1969).
2. A.K.L. Fan, G.H. Rosenthal, H.L. McKinzie, and A. Wold: Preparation and properties of $FeAs_2$ and $FeSb_2$. *J. Solid State Chem.* **5**, 136 (1972).
3. J. Steger and E. Kostiner: Mossbauer effect study of $FeSb_2$. *J. Solid State Chem.* **5**, 131 (1972).
4. C. Petrovic, J.W. Kim, S.L. Bud'ko, A.I. Goldman, and P.C. Canfield: Anisotropy and large magnetoresistance in the narrow-gap semiconductor $FeSb_2$. *Phys. Rev. B* **67**, 155205 (2003).
5. A. Bentien, S. Johnsen, G.K.H. Madsen, B.B. Iversen, and F. Steglich: Colossal Seebeck coefficient in strongly correlated semiconductor $FeSb_2$. *Euro. Phys. Lett.* **80**, 17008 (2007).
6. H. Zhao, M. Pokharel, G. Zhu, S. Chen, K. Lukas, J. Qing, C. Opeil, G. Chen, and Z. Ren: Dramatic thermal conductivity reduction by nanostructures for large increase in thermoelectric figure-of-merit of $FeSb_2$. *Appl. Phys. Lett.* **99**, 163101 (2011).
7. C. Herring: Theory of the thermoelectric power of semiconductors. *Phys. Rev.* **96**, 1163 (1954).
8. T.H. Geballe and G.W. Hull: Seebeck effect in silicon. *Phys. Rev.* **94**, 1134 (1954).
9. P. Sun, N. Oeschler, S. Johnsen, B.B. Iversen, and F. Steglich: Narrow band gap and enhanced thermoelectricity in $FeSb_2$. *Dalton Trans.* **39**, 1012 (2010).
10. P. Sun, N. Oeschler, S. Johnsen, B.B. Iversen, and F. Steglich: $FeSb_2$: prototype of huge electron-diffusion thermoelectricity. *Phys. Rev. B* **79**, 153308 (2009).
11. A. Bentien, G.K.H. Madsen, S. Johnsen, and B.B. Iversen: Experimental and theoretical investigations of strongly correlated $FeSb_{2-x}Sn_x$. *Phys. Rev. B* **74**, 205105 (2006).
12. P. Sun, M. Søndergaard, Y. Sun, S. Johnsen, B.B. Iversen, and F. Steglich: Unchanged thermopower enhancement at the semiconductor-metal transition in correlated $FeSb_{2-x}Te_x$. *Appl. Phys. Lett.* **98**, 072105 (2011).
13. H. Takahashi, R. Okazaki, Y. Yasui, and I. Terasaki: Low-temperature magnetotransport of narrow-gap semiconductor $FeSb_2$. *Phys. Rev. B* **84**, 205215 (2011).
14. J.M. Tomczak, K. Haule, T. Miyake, A. Georges, and G. Kotliar: Thermopower of correlated semiconductors: application to $FeAs_2$ and $FeSb_2$. *Phys. Rev. B* **82**, 085104 (2010).
15. N. Kh. Abrikosov and L.I. Petrova: The polythermal cross-section $FeSb_2$-$FeTe_2$ of the Fe-Sb-Te system. *Inorg. Mater.* **25**, 1087 (1989).
16. Y. Sun, S. Johnsen, P. Eklund, M. Sillassen, J. Bøttiger, N. Oeschler, P. Sun, F. Steglich, and B.B. Iversen: Thermoelectric transport properties of highly oriented $FeSb_2$ thin films. *J. Appl. Phys.* **106**, 033710 (2009).

https://doi.org/10.1557/mrc.2013.7 Published online by Cambridge University Press

17. L. Weber, M. Lehr, and E. Gmelin: Reduction of the thermopower in semiconducting point contacts. *Phys. Rev. B* **46**, 9511 (1992).
18. F.J. Blatt: *Physics of Electronic Conduction in Solids* (McGraw-Hill, New York, NY, 1968).
19. Q.R. Hou, B.F. Gu, Y.B. Chen, and Y.J. He: Phonon-drag effect of ultrathin $FeSi_2$ and $MnSi_{1.7}/FeSi_2$ films. *Mod. Phys. Lett. B* **25**, 1829 (2011).
20. J.P. Issi and J. Boxus: Phonon-drag low temperature refrigeration. *Cryogenics* **19**, 517 (1979).
21. L. Weber and E. Gmelin: Transport properties of silicon. *Appl. Phys. A* **53**, 136 (1991).
22. A. Perucchi, L. Degiorgi, R. Hu, C. Petrovic, and V.F. Mitrović: Optical investigation of the metal-insulator transition in $FeSb_2$. *Eur. Phys. J., B* **54**, 175 (2006).
23. N. Lazarević, Z.V. Popović, R. Hu, and C. Petrovic: Evidence for electron-phonon interaction in Fe_{1-x} M_xSb_2 (M = Co and Cr; $0 \leq x \leq 0.5$) single crystals. *Phys. Rev. B* **81**, 144302 (2010).
24. D.T. Morelli: Phonon-drag thermopower. Ph.D. Dissertation. University of Michigan, 1985., p. 82.
25. J. Tang, W. Wang, G.L. Zhao, and Q. Li: Colossal positive Seebeck coefficient and low thermal conductivity in reduced TiO_2. *J. Phys. Condens. Matter* **21**, 205703 (2009).
26. C. Petrovic, Y. Lee, T. Vogt, Dj.N. Lazarov, S.L. Bud'ko, and J. Canfield: Kondo insulator description of spin state transition in $FeSb_2$. *Phys. Rev. B* **72**, 045103 (2005).
27. J. Ziman: *Electrons and Phonons* (Oxford University Press, Oxford, UK, 2001).
28. W.R. Thurber and A.J.H. Mante: Thermal conductivity and thermoelectric power of rutile (TiO_2). *Phys. Rev.* **139**, A1655 (1965).
29. R.W. Keyes: *Thermoelectricity: Science and Engineering*, edited by R.R. Heikes and R.W. Ure Jr., (Interscience, New York, 1961).
30. H.J. Goldsmid: *Introduction to Thermoelectricity: Springer Series in Material Science* (Springer-Verlag, Berlin, Germany, 2010).
31. Y.U.V. Ivanov: *Thermoelectric Handbook: Macro to Nano*, edited by D.M. Rowe (CRC Taylor and Francis, Boca Raton, FL, 2006).
32. A.D. Becke: A new mixing of Hartree–Fock and local density – functional theories. *J. Chem. Phys.* **98**, 1372 (1993).
33. L. Hedin: New method for calculating the one-particle Green's function with application to the electron-gas problem. *Phys. Rev.* **139**, A796 (1965).
34. H.P.R. Frederikse and E.V. Mielczarek: Thermoelectric power of indium antimonide. *Phys. Rev.* **99**, 1889 (1955).

https://doi.org/10.1557/mrc.2013.7 Published online by Cambridge University Press